α-Aminobisphosphonate Copolymers Based on Poly(ϵ-caprolactone)s and Poly(ethylene glycol): A New Opportunity for Actinide Complexation

Carlos Arrambide, Loona Ferrie, Benedicte Prelot, Amine Geneste, Sophie Monge, Vincent Darcos

α-Aminobisphosphonate copolymers based on poly(ε-caprolactone)s and poly(ethylene glycol): a new opportunity for actinide complexation

Carlos Arrambide,[1] *Loona Ferrie,*[2] *Benedicte Prelot,*[2] *Amine Geneste,*[2] *Sophie Monge,*[2]* *and Vincent Darcos*[1]*

[1] IBMM, Univ Montpellier, CNRS, ENSCM, Montpellier, France

[2] ICGM, Univ Montpellier, CNRS, ENSCM, Montpellier, France

KEYWORDS. Actinides, bisphosphonate, complexation, ITC, cerium, neodymium

ABSTRACT. Original α-aminobisphosphonate-based copolymers were synthesized and successfully used for actinide complexation. For this purpose, poly(α-chloro-ε-caprolactone-*co*-ε-caprolactone)-*b*-poly(ethylene glycol)-*b*-poly(α-chloro-ε-caprolactone-*co*-ε-caprolactone) (P(αClεCL-*co*-εCL)-*b*-PEG-*b*-P(αClεCL-*co*-εCL)) copolymers were first prepared by ring-opening copolymerization of ε-caprolactone (εCL) and α-chloro-ε-caprolactone (αClεCL) using poly(ethylene glycol) (PEG) as macro-initiator and tin(II) octanoate as catalyst. The chloride functions were then converted to azide moieties by chemical modification, and finally α-aminobisphosphonate alkyne ligand (TzBP) was grafted using click chemistry, to afford well-defined poly(αTzBPεCL-*co*-εCL)-*b*-PEG-*b*-poly(αTzBPεCL-*co*-εCL) copolymers. Three copolymers, showing different α-aminobisphosphonate group ratios, were prepared (7, 18, and 38%), namely CP8, CP9 and CP10, respectively. They were characterized by ^{1}H and ^{31}P NMR, and size exclusion chromatography. Sorption properties of these copolymers were evaluated by Isothermal Titration Calorimetry (ITC) with neodymium (Nd(III)) and cerium (Ce(III)) cations, used as surrogates of actinides, especially uranium and plutonium, respectively. ITC enabled the determination of the full thermodynamic profile, and the calculation of the complete set of thermodynamic parameter (ΔH, $T\Delta S$, ΔG), with the K_a constant and the n stoichiometry. The results showed that the number of cations sorbed by the functional copolymers logically increased with the number of bisphosphonate functions borne by the macromolecular chain, independently of the complexed cation. Additionally, CP9 and CP10 copolymers showed higher sorption capacities (21.4 and 34.0 $mg.g^{-1}$ for Nd(III) and 9.6 and 14.3 $mg.g^{-1}$ for Ce(III), respectively) than most of the systems previously described in the literature. CP9 also showed a highest binding constant (7000 M^{-1}). These copolymers, based on non-toxic and biocompatible poly(ε-caprolactone) and poly(ethylene glycol) are of great interest for external

body decontamination of actinides as they combine high number of complexing groups, thus leading to great decontamination efficiency, and limited diffusion through the skin due to their high molecular weight, thus avoiding additional possible internal contamination.

INTRODUCTION

Over the last few decades, the use of actinides in areas such as nuclear, military and medical fields has led to risks of environmental and health contaminations. Indeed, actinides being radioactive elements, their isotopes are all unstable and decay by emitting high-energy particles or radiation, which causes great damage. Among these elements, thorium (Th) and uranium (U) are the most abundant. The controlled use of these emitted radiations was applied in many fields, such as the nuclear industry, military or medical sectors. In particular, nuclear power plants employed ^{235}U and ^{239}Pu to generate electric power[1] while the explosive power of enriched uranium was used to make atomic bombs.[2, 3] Furthermore, the medical sector employed actinides in cancer therapy or as markers to follow the path of an active substance in the body.[4, 5] Additionally, ^{238}Pu was used in heart pacemakers to power them to work for at least 10 years.[6] All these uses are source of risks, accidents and contamination of the population. When contaminated, actinides can cause skin burns and diffuse through the skin barrier into the bloodstream or enter the body by inhalation or ingestion. Once in the body, the radioelements usually pass through the bloodstream to be distributed in the body and accumulate in the organs and bones, causing significant damage due to their radioactivity. For instance, some actinides can be found in the lungs, the skeleton or in the kidneys,[7] and are the cause of many diseases such as multiple cancers, cardiovascular problems, nervous system disorders, or fertility problems.[8, 9]

In that context, the novelty of the work described here is the synthesis of well-defined copolymers based on non-toxic and biocompatible polymers bearing high number of bisphosphonic acid moieties able to efficiently complex actinides that could be used for body decontamination purposes. Currently, solutions allowing internal or external decontamination

are still rare, and developed systems are not very efficient, showing many drawbacks and health risks for contaminated people. In a general manner, employed derivatives for decontamination must be non-toxic, and ensure fast sorption with great affinity for actinides, thus forming a stable complex with toxic metallic cations to efficiently extract them. Nowadays, to the best of our knowledge, except the hydroxypyridonates (HOPO),[10] β-dicarbonyl(bis-catecholamine)[11] or terephthalamide (TAM)/maltolamide (MAM)[12] hexadentate ligands recently developed, efficient molecules for radionuclide decontamination, such as thorium, uranium, neptunium or plutonium, bore acidic moieties (mainly carboxylic, or phosphonic acid groups, more rarely sulfonic group).[13, 14] Concerning carboxylic acids, diethylenetriaminepentaacetic acid (DTPA) was considered for plutonium/uranium complexation.[15] In particular, diethylenetriaminepentaacetic acid trisodium calcium and trisodium zinc salts (Ca-DTPA and Zn-DTPA) chelating ligands, approved by the *Food and Drug Administration*, showed some risks when frequently used because they complexed other elements essential to the human body than actinides.[16] Carboxylic acidic based-calixarene were also employed, and proved to be good chelating agents for uranium but still remain expensive.[17-19] Side to carboxylic acids, sulfonic acid-based molecules were scarcely considered. For instance, sulfonic-based catecholates were developed but were less efficient than HOPO derivatives.[13] Globally, all considered developed molecules were more or less appropriate for *in vivo* applications due to their toxicity and the side effects they led to.

Last acid-based molecules that were studied for body decontamination were bisphosphonic acid ones. The latter bore two complexing groups, thus rationally increasing their sorption efficiency. Some examples involving these functional groups demonstrated their effectiveness with promising capacities of actinides chelation, notably in the case of uranium sorption.[20]

Indeed, ethane-1-hydroxy-1,1-bisphosphonate (EHBP), also known as etidronic acid, showed very valuable results for complexation and was well tolerated by the organism.[21] It was for instance employed for the removal of uranium after intramuscular injection as a simulated wound intake in rats.[22] The administration of this chelating agent proved to be effective in decreasing the concentration in kidneys, bone, and liver, and the lethal effect in mice contaminated with uranium. This molecule was even commercialized under the name of Didronel®. In another example, aldehyde-bisphosphonate conjugates have been described for the complexation of uranyl ions, showing excellent sorption capacities of these cations under mild conditions.[23] Finally, molecules bearing a higher number of bisphosphonated functional complexing groups were developed such as a tetraphosphonate or a bisphosphonate trifunctional molecules,[24] a polyphosphorylated calix[4]arene bearing four bisphosphonic acid moieties,[25] and magnetite nanoparticles modified by bisphosphonates.[26] All these multifunctional molecules were used for internal decontamination and appeared as good chelating agents toward uranium. In contrast, such derivatives were toxic and could bioacculumate in blood, which was problematic. Nevertheless, even if these last examples showed important drawbacks, they highlighted the interest of developing multifunctional complexing molecules to favor uranium complexation.

From a more general point of view, decorporation ligands still suffer nowadays from drawbacks of high toxicity, fast metabolism, or limited removal ability.[13, 27] Therefore, new possibilities with the development of optimized and less toxic systems are highly desired. In that context, the objective of the reported work is the synthesis of non-toxic breakthrough macromolecules allowing efficient and rapid complexation of actinides, in particular uranium element, to successfully overcome external contamination. In this particular case, the most

conventional procedure employed is a simple rinsing of the contaminated skin with soap and water. Unfortunately, this technique has a limited effectiveness because no specific complexing group is involved and, as a result, it is far from being sufficient to extract all the actinides deposited on the skin. Additionally, this procedure does not allow eliminating the absorbed elements. Thus, it appears of great interest to develop new efficient external decontamination systems able to remove very high quantity of radioactive elements, and to prevent their penetration into the body after criminal or accidental contamination, without inducing additional toxicity. So, the concept developed in this contribution lied on the use of functionalized non-toxic and biocompatible polymers with limited cost bearing high number of bisphosphonic acid moieties. For such purpose, an α-aminobisphosphonate alkyne complexing ligand was first synthesized. To be more efficiently used for external decontamination, this ligand was grafted onto a polymer to obtain a high molecular weight material bearing a high number of complexing moieties and not able to penetrate the skin barrier. Poly(ε-caprolactone) (PεCL) was chosen for the synthesis of different copolymers because of its biocompatibility and the versatile possibility of grafting ligands onto its linear chain. As PεCL is not soluble in water, poly(ethylene glycol) (PEG) was involved to form water soluble PεCL-*b*-PEG-*b*-PεCL based decontaminating materials, with a controlled amount of bisphosphonate ligand. PEG has already been used for biomedical applications due to its low toxicity and biocompatibility.[28] Combination of PεCL and PEG segments allowed obtaining systems, which were already widely used in the medical field, especially for drug delivery.[29-31] In order to graft the bisphosphonate ligand onto PεCL, a chlorinated copolymer, namely poly(α-chloro-ε-caprolactone-*co*-ε-caprolactone)-*b*-poly(ethylene glycol)-*b*-poly(α-chloro-ε-caprolactone-*co*-ε-caprolactone), was first prepared by ring-opening polymerization of ε-caprolactone and α-chloro-ε-caprolactone. In a second step, chloride groups of PεCL were substituted by azide groups using sodium azide as nucleophilic agent.

Amino bisphosphonate copolymers were then synthesized by click chemistry reaction of the preformed azido-functionalized copolyester with the alkyne-functionalized bisphosphonate developed. Click chemistry, widely used in the synthesis of many functionalized polymers,[32, 33] guaranteed a high yield and purity of the synthesized products, required mild reaction conditions, and did not produce little by-products.[34] The interest of our synthetic pathway is that it allowed an easy introduction of bisphosphonate-based ligands, which are known to be quite difficult to prepare. It was also possible to easily vary the number of complexing groups using click chemistry, thus adapting our system to actinide concentration to be sorbed. Introduction of different alkyne-based ligands could also be considered, to selectively and efficiently complex different actinides. Finally, sorption properties of the developed copolymers (constant and stoichiometry) were studied by Isothermal Titration Calorimetry (ITC) using lanthanides (neodymium and cerium), surrogates of actinides. Obtained results were compared to those obtained for other systems described in the literature.[35]

EXPERIMENTAL SECTION

Materials and Methods. Chemicals and solvents were purchased from Sigma-Aldrich, and were used without further purification unless otherwise stated. ε-Caprolactone, toluene and N,N-dimethylformamide (DMF) were dried over calcium hydride for 24 hours at room temperature and distilled under reduced pressure. Poly(ethylene glycol) (M_n=1000 g.mol^{-1}, Sigma-Aldrich) was dried by azeotropic distillation with toluene. Aqueous solutions were prepared with Milli-Q water of 18.2 MΩ.cm. α-Chloro-ε-caprolactone (αClεCL) and acetylenic aminobisphosphonate were prepared as previously reported by Lenoir *et al.*[36] and Cavero *et al.*,[37] respectively.

Characterization.

Nuclear Magnetic Resonance spectroscopy (NMR). ^{1}H NMR spectra were recorded on a Bruker spectrometer (AMX300) operating at 300 MHz. Deuterated chloroform was used as solvent, and chemical shifts were referenced to the peak of the residual non-deuterated solvent.

Synthesis of poly(α-chloro-ε-caprolactone-co-*ε-caprolactone)*-b-*poly(ethylene glycol)*-b-*poly(α-chloro-ε-caprolactone*-co-*ε-caprolactone) (P(αClεCL*-co-*εCL)-PEG-P(αClεCL*-co-*εCL).* The experimental molar ratio ($F_{\alpha Cl\varepsilon CL}$) of the α-chloro-ε-caprolactone (αClεCL) in the copolymers was determined by ^{1}H NMR (**Equation 1**) from the characteristic signals of each monomeric unit at δ 4.00-4.30 ppm for αClεCL ($^1/_3\,[I_{AEe} - I_a]$) and at δ 2.30 ppm for εCL (I_a).

$$F_{\alpha Cl\varepsilon CL} = \frac{^1/_3\,[I_{AEe} - I_a]}{^1/_3\,[I_{AEe} - I_a] + ^1/_2\,I_a} \qquad \textbf{(Equation 1)}$$

The experimental molecular weight ($M_{n,NMR}$) was determined by ^{1}H NMR (**Equation 2**) from the characteristic signals of each monomeric unit at δ 4.00-4.30 ppm for αClεCL ($^1/_3\,[I_{AEe} - I_a]$), at δ 2.30 ppm for εCL (I_a) and at δ 3.63 ppm for PEG (I_m).

$$M_{n,NMR} = M_{n,PEG} + \frac{^1/_3[I_{AEe} - I_a]\times 149 + {}^1/_2 I_a \times 114}{^1/_{85} I_m} \qquad \textbf{(Equation 2)}$$

Synthesis of poly(α-azido-ε-caprolactone-co-*ε-caprolactone)*-b-*poly(ethylene glycol)*-b-*poly(α-azido-ε-caprolactone*-co-*ε-caprolactone) (poly(αN$_3$εCL*-co-*εCL)*-b-*PEG*-b-*poly(αN$_3$εCL*-co-*εCL)) copolymers.* The experimental molar ratio ($F_{\alpha N3\varepsilon CL}$) of α-azido-ε-caprolactone (αN$_3$εCL) in the copolymers was determined by ^{1}H NMR (**Equation 3**) from the characteristic signals of each monomeric unit at δ 3.8 ppm for αN$_3$εCL (I_A) and at δ 2.30 ppm for εCL (I_a).

$$F_{\alpha N3\varepsilon CL} = \frac{I_A}{I_A + {}^1/_2\, I_a} \qquad \textbf{(Equation 3)}$$

The experimental molecular weight ($M_{n,NMR}$) was determined by ^{1}H NMR (**Equation 4**) from the characteristic signals of each monomeric unit at δ 3.80 ppm for αN$_3$εCL (I_A), at δ 2.30 ppm for εCL (I_a) and at δ 3.63 ppm for PEG (I_m).

$$M_{n,NMR} = M_{n,PEG} + \frac{I_A \times 454 + {}^1/_2\, I_a \times 114}{^1/_{85}\, I_m} \qquad \textbf{(Equation 4)}$$

Synthesis of (αTzBPεCL-co-*εCL)*-b-*PEG*-b-*poly(αTzBPεCL*-co-*εCL) α-aminobisphosphonate-based copolymers.* The experimental molar ratio ($F_{\alpha TzBP\varepsilon CL}$) of the bisphosphonate ligand (αTzBP$_3$εCL) in the copolymers (**Equation 5**) was determined by ^{1}H NMR from the characteristic signals of each monomer units at δ 3.71 ppm for αTzBP$_3$εCL (I_r) and at δ 2.30 ppm for εCL (I_a).

$$F_{\alpha TzBP\varepsilon CL} = \frac{^1/_{12}\, I_r}{^1/_{12}\, I_r + {}^1/_2\, I_a} \qquad \textbf{(Equation 5)}$$

The experimental molecular weight ($M_{n,NMR}$) was determined by ^{1}H NMR (**Equation 6**) from the characteristic signals of each monomeric unit at δ 3.71 ppm for αTzBP$_3$εCL (I_r), at δ 2.30 ppm for εCL (I_a) and at δ 3.63 ppm for PEG (I_m).

$$M_{n,NMR} = M_{n,PEG} + \frac{{}^{1}/_{12}\, I_r \times 155 + {}^{1}/_{2}\, I_a \times 114}{{}^{1}/_{85}\, I_m} \qquad \textbf{(Equation 6)}$$

FTIR spectroscopy. Infrared spectra were recorded on a Perkin-Elmer Spectrum 100 FTIR spectrometer.

Size exclusion chromatography (SEC). SEC was performed using a Shimadzu Prominence system (Shimadzu Corp, Kyoto, Japan) equipped with a PLgel Mixed-C guard column (Agilent, 5 µm, 50 x 7.5 mm), two mixed medium columns PLgel Mixed-C (5 µm, 300 x 7.8 mm) and a Shimadzu RI detector 20 A. The mobile phase was THF with a flow of 1 mL.min^{-1} at 35 °C. Polystyrene standards were used for calibration and polymer characteristics (M_n, M_w, $Đ$) were obtained according to those standards.

Isothermal Titration Calorimetry (ITC). ITC measurements were performed with a TAM III multichannel calorimetric device having a Micro Reaction System and a dedicated twin channel Nanocalorimeters, with sinks containing the reference and the sample ampoules (TA Waters). All the experiments were carried out at a temperature equal to 25 °C, in cells (hastelloy) containing 800 µL of the polymer solution. An ITC experiment comprised 25 injections of 10 seconds of 10 µL of cation solution. These injections were spaced 45 min apart in order to allow the system stabilizing between two injections, and the latter was agitated thanks to a gold paddle stirrer at 45 rpm.

Synthesis of copolymers.

Typical procedure for the synthesis of poly(α-chloro-ε-caprolactone-co-*ε-caprolactone)*-b-*poly(ethylene glycol)*-b-*poly(α-chloro-ε-caprolactone*-co-*ε-caprolactone) (P(αClεCL*-co-*εCL)*-b-*PEG*-b-*P(αClεCL*-co-*εCL)) (CP3 copolymer).* Ring opening polymerization was carried out in toluene solution using standard Schlenk technique under an inert atmosphere of argon. ε-Caprolactone (3.42 g, 30 mmol, 15 equiv.), α-chloro-ε-caprolactone[36] (1.48 g, 10 mmol, 5 equiv.), tin octanoate ($Sn(Oct)_2$) (324 mg, 0.8 mmol, 0.4 equiv.), PEG (M_n = 1000 $g.mol^{-1}$, 2 g, 2 mmol, 1 equiv.), and anhydrous toluene (15 mL) were placed in an oven-dried Schlenk tube. The tube was fitted with a rubber septum. The solution was further degassed by three freeze-pump-thaw cycles. The resulting mixture was stirred at 100 °C for 24 hours. The reaction was stopped by addition of an excess of 1 N HCl. The reaction mixture was then poured into cold diethyl ether. The precipitated polymer was finally collected by filtration and dried *in vacuo* to yield 5.24 g of copolymer (yield: 76 %). ^{1}H NMR ($CDCl_3$): δ ppm 4.32 (m, P(αClεCL)-O-CH_2), 4.26 (t, C*H*Cl), 4.17 (m, O-CH_2-$(CH_2)_3$-CHCl), 4.06 (m, O-CH_2-$(CH_2)_4$), 3.65 (m, O-$(CH_2)_2$-O), 2.30 (t, C(O)-CH_2), 1.75-1.3 (m, O-CH_2-$(CH_2)_3$). $M_{n,SEC}$ = 5500 $g.mol^{-1}$, $Đ$ = 1.42.

Typical procedure for the synthesis of poly(α-azido-ε-caprolactone-co-*ε-caprolactone)*-b-*poly(ethylene glycol)*-b-*poly(α-azido-ε-caprolactone*-co-*ε-caprolactone) (P(αN₃εCL*-co-*εCL)*-b-*PEG*-b-*P(αN₃εCL-co-εCL)) (CP7 copolymer).* P(αClεCL-*co*-εCL)-*b*-PEG-*b*-P(αClεCL-*co*-εCL) (CP3, 1 g, 3100 $g.mol^{-1}$, 3.05×10^{-3} mole equiv. of αClεCL), sodium azide (1 g, 3.05×10^{-2} mole, 10 equiv.) and DMF (10 mL) were added in a round bottom flask. The mixture solution was stirred at room temperature overnight. After elimination of DMF *in vacuo*, toluene was added, and the insoluble salts were removed by filtration over celite. After

solvent evaporation, the polymer was recovered by precipitation in cold diethyl ether (yield: 94 %). ^{1}H NMR ($CDCl_3$): δ ppm 4.32 (m, P(αN$_3$εCL)-O-C*H*$_2$), 4.17 (m, O-C*H*$_2$-(CH$_2$)$_3$-CHN$_3$), 4.06 (m, O-C*H*$_2$-(CH$_2$)$_4$), 3.83 (m, C*H*N$_3$), 3.65 (m, O-(C*H*$_2$)$_2$-O), 2.30 (t, C(O)-C*H*$_2$), 1.75-1.3 (m, O-CH$_2$-(C*H*$_2$)$_3$). $M_{n,SEC}$ = 5400 g.mol^{-1}, $Đ$ = 1.41.

*Typical procedure for the synthesis of α-aminobisphosphonate-based copolymers (αTzBPεCL-*co*-εCL)-b-PEG-b-poly(αTzBPεCL-co-εCL) (CP10 copolymer).* In Schlenk tube A were placed the P(αN$_3$εCL-*co*-εCL)-*b*-PEG-*b*-P(αN$_3$εCL-*co*-εCL) copolymer (CP7, 0.9 g, 2.24×10^{-3} mole equiv. of azide), the acetylenic aminobisphosphonate (0.74 g, 2.46×10^{-3} mole, 1.1 equiv.), pentamethyldiethylenetriamine (PMDETA) (0.85 g, 2.23×10^{-3} mole, 1 equiv), and DMF (5 mL). The tube was fitted with a rubber septum and the solution was further degassed by three freeze-pump-thaw cycles. A second Schlenk tube B containing copper (I) bromide (CuBr) (0.35 g, 2.46×10^{-3} mole, 1.1 equiv) was degassed and placed under an argon atmosphere. Then, the solution of tube A was transferred by canula to the tube B. The solution was stirred at room temperature for 24 hours. The solution was then passed through a basic alumina column to remove copper salt. After solvent evaporation, the polymer was recovered by precipitation in cold diethyl ether (yield: 52%). ^{1}H NMR ($CDCl_3$): δ ppm 7.86 (m, N-C*H*=C), 5.27 (m, C*H*TzBP), 4.27 (m, P(αTzBPεCL)-O-C*H*$_2$), 4.10 (m, O-C*H*$_2$-(CH$_2$)$_3$-CHTzBP), 4.00 (m, O-C*H*$_2$-(CH$_2$)$_4$), 3.73 (d, P-O-C*H*$_3$), 3.60 (m, O-(C*H*$_2$)$_2$-O), 3.13 (d, N-C*H*$_2$-P), 2.23 (m, C(O)-C*H*$_2$), 1.60-1.32 (m, O-CH$_2$-(C*H*$_2$)$_3$). ^{31}P NMR (300 MHz, $CDCl_3$): δ ppm 26.46 (s, 2P).

Solutions for Isothermal Titration Calorimetry. The concentration of the solutions (cation and polymer) was optimized after several tests to properly detect the heat flow signal,

to assess the important inflexion including the end of the process, and thus to get appropriate data for further calculation. In all cases, aqueous solutions of polymers or cations were prepared by dissolving in Milli-Q water to achieve the desired concentration. Subsequently, the pH of these solutions was adjusted to reach 5.5 with 0.5 $mol.L^{-1}$ HNO_3 solution or 0.5 $mol.L^{-1}$ NaOH solution. The set of conditions for the polymer and the cation aqueous solutions are the following. CP8, CP9 and CP10 copolymer solutions were prepared at concentrations equal to 5 $g.L^{-1}$, 1.3 $g.L^{-1}$ and 1.3 $g.L^{-1}$, respectively. The cation aqueous solutions (Nd(III) neodymium and Ce(III) cerium) were prepared by dissolving neodymium(III) nitrate hexahydrate or cerium(III) nitrate hexahydrate, and the concentrations used for CP8, CP9 and CP10 were 3 mM, 3 mM and 6 mM, respectively.

RESULTS AND DISCUSSION

The synthesis of α-aminobisphosphonate-based copolymers, namely poly(αTzBPεCL-*co*-εCL)-*b*-PEG-*b*-poly(αTzBPεCL-*co*-εCL) copolymers, was achieved following a three step synthesis procedure (**Scheme 1**), using α-chloro-ε-caprolactone (αClεCL), preliminary prepared according to work already described in the literature.[36]

Scheme 1. Synthetic pathway for the synthesis of poly(αTzBPεCL-*co*-εCL)-*b*-PEG-*b*-poly(αTzBPεCL-*co*-εCL) complexing copolymers

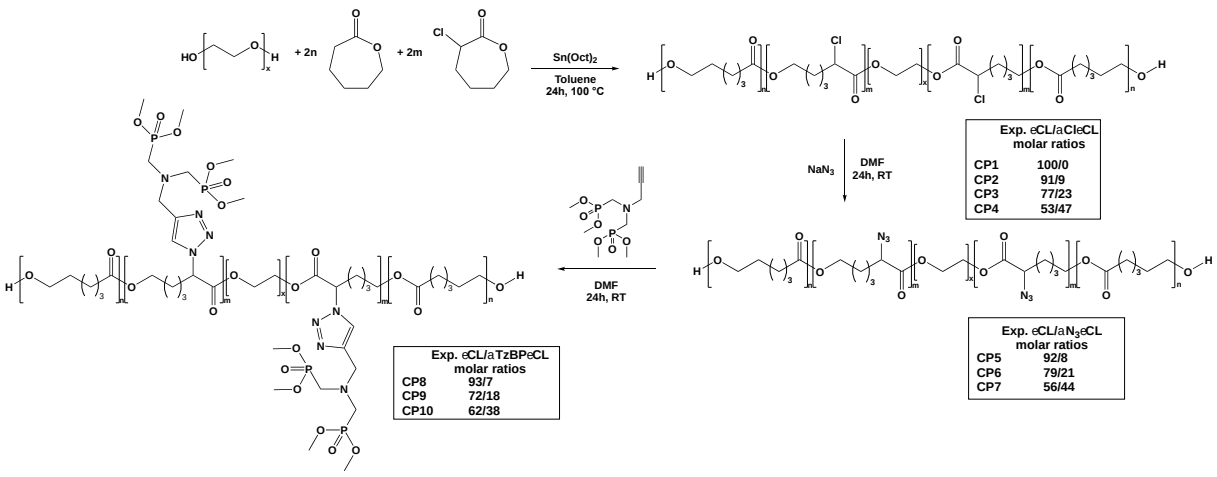

Synthesis of poly(αClεCL-*co*-εCL)-*b*-PEG-*b*-poly(αClεCL-*co*-εCL) copolymers. The synthesis of α-chloro-ε-caprolactone (αClεCL) was first performed by oxidation of α-chlorocyclohexanone using *m*-peroxybenzoic acid according to procedure previously described in the literature by Lenoir *et al* (**Scheme S1**).[36] αClεCL was prepared in large scale (25-50 grams) and stored for a few weeks at -15 °C without significant loss of polymerizability. The ^{1}H NMR spectrum of αClεCl was consistent with the assigned structure (**Figure S1**). Then, a series of poly(αClεCL-*co*-εCL)-*b*-PEG-*b*-poly(αClεCL-*co*-εCL) triblock copolymers based on ε-caprolactone (εCL) and poly(ethylene glycol) (PEG) containing different theoretical molar ratios ($f_{\alpha Cl\varepsilon CL}$) of αClεCL were prepared by ring-opening

copolymerization of αClεCL and εCL using PEG (M_n = 1000 g.mol^{-1}) as initiator and tin 2-ethylhexanoate as catalyst in toluene solution at 100 °C (**Scheme 1**). After 24 hours polymerization, conversions of both monomers, determined by ^{1}H NMR, were quantitative. After purification by precipitation in cold diethyl ether, the chlorinated copolymers were characterized by ^{1}H NMR and size exclusion chromatography (SEC). **Table 1** summarizes the characteristics of the four prepared (co)polymers with theoretical molar ratio $f_{\alpha Cl\varepsilon CL}$ and molar masses ranging from 0 to 50%, and from 3300 to 3600 g.mol^{-1}, respectively. Four different εCL/αClεCL molar ratios were targeted, equal to 100/0, 90/10, 25/75, and 50/50, leading to CP1, CP2, CP3, and CP4 copolymers, respectively. ^{1}H NMR spectra (**Figure 1** and **Figure S2**) showed peaks corresponding to both monomeric units, especially at 4.32, 4.26 and 3.30 ppm, for the methine bearing the chlorine atom of the αClεCL, the methylene of the ethylene glycol unit, and the methylene in the α-position of the carbonyl group in the εCL, respectively.

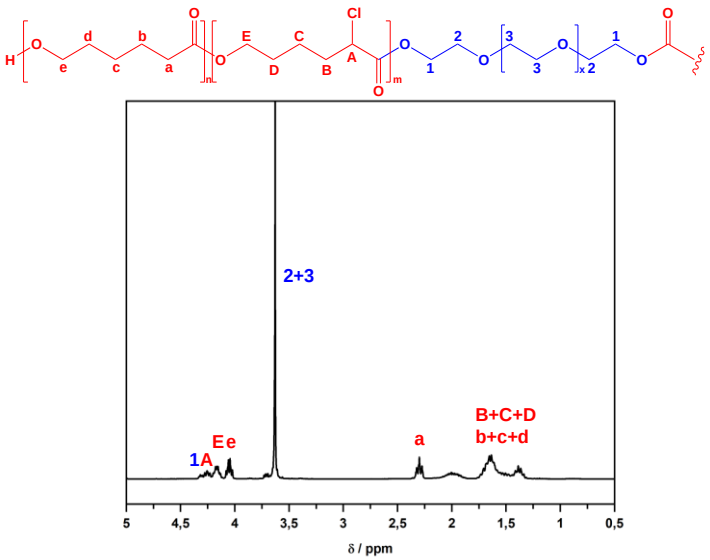

Figure 1. ^{1}H NMR spectrum in deuterated chloroform of poly(αClεCL-*co*-εCL)-*b*-PEG-*b*-poly(αClεCL-*co*-εCL) (CP3); $F_{\alpha Cl\varepsilon CL}$ = 0.23.

^{1}H NMR spectroscopy also allowed determining the experimental molar ratio in αClεCL monomer ($F_{\alpha Cl\varepsilon CL}$) and the molecular weight ($M_{n,NMR}$), comparing peaks at δ 4.00 and 2.29 ppm assigned to εCL monomeric units and peaks at δ 4.10 and 4.25 ppm corresponding to the chlorinated εCL monomer. Integrations of protons of εCL monomer logically decreased going from CP2 to CP4 (**Figure S2**), thus demonstrating the incorporation of increasing amount of αClεCL in the copolymers. This was also confirmed by the increase of the integrations at δ 4.10 and 4.25 ppm, attributed to protons of the chlorinated monomer. Additionally, experimental molecular composition in chlorinated caprolactone ($F_{\alpha Cl\varepsilon CL}$) was calculated from the relative intensity of the ^{1}H NMR signals of the αClεCL and αCL monomeric units (**Table 1**, **Equation 1**). Experimental $F_{\alpha Cl\varepsilon CL}$ were close from theoretical values, varying from 0.09 to 0.47 (CP2 to CP4), which was consistent with a good and controlled incorporation of chlorinated caprolactone during the polymerization. The molecular weights ($M_{n,NMR}$) of chlorinated copolyesters were calculated from the relative intensity of the ^{1}H NMR signals of both caprolactone and ethylene glycol monomer unit (**Table 1**, **Equation 2**). Once again, the experimental values were close from the theoretical ones. Finally, size exclusion chromatography (SEC) traces of the copolymers displayed monomodal and narrow signals, consistent with a well-controlled polymerization process (**Figure S3**). SEC traces of the chlorinated copolymers showed a slight shift toward higher molecular weight in comparison with PεCL. Elution time also increased with chlorinated monomeric unit molar ratio. No residual PEG was observed.

Table 1. Characteristics of poly(εCL)-*b*-PEG-*b*-poly(εCL) (CP1) and poly(αClεCL-*co*-εCL)-*b*-PEG-*b*-poly(αClεCL-*co*-εCL) copolymers (CP2, CP3, CP4) synthesized by ring-opening polymerization[a]

Copolymer	$[\varepsilon CL]_0/[\alpha Cl\varepsilon CL]_0$	$f_{\alpha Cl\varepsilon CL}$[b]	$F_{\alpha Cl\varepsilon CL}$[c]	Yield (%)	$M_{n,th}$[d] ($g.mol^{-1}$)	$M_{n,NMR}$[e] ($g.mol^{-1}$)	$M_{n,SEC}$[f] ($g.mol^{-1}$)	$Đ$[f]
CP1	100/0	0	0	82	3300	3400	4600	1.27
CP2	90/10	0.10	0.09	73	3350	3200	5200	1.30
CP3	75/25	0.25	0.23	76	3450	3100	5500	1.42
CP4	50/50	0.5	0.47	69	3600	3700	5100	1.43

[a] Conditions of ROP: $[PEG]/[Sn(Oct)_2] = 1/0.4$, $M_{n,PEG} = 1000$ $g.mol^{-1}$, solvent: toluene, T = 100 °C, time of polymerization = 24 hours; [b] $f_{\alpha Cl\varepsilon CL} = DP_{\alpha Cl\varepsilon CL} / (DP_{\alpha Cl\varepsilon CL}+DP_{\varepsilon CL})$; [c] calculated from **Equation 1**; [d] $M_{n,th} = M_{n,PEG} + [(([\alpha Cl\varepsilon CL]_0/[PEG]_0) \times 149) + (([\varepsilon CL]_0/[PEG]_0) \times 114)]$; [e] calculated from **Equation 2**; [f] determined by SEC in THF using polystyrene standards.

Synthesis of poly(αN3εCL-*co*-εCL)-*b*-PEG-*b*-poly(αN3εCL-*co*-εCL) copolymers. In a second step, azide-functionalized copolymers were prepared by chemical modification of previously synthesized copolymers (CP2, CP3, and CP4). The chlorine pendent groups of αClPεCL were converted into azido groups by nucleophilic substitution using sodium azide (NaN_3) in DMF at room temperature, yielding to a series of poly(αN3εCL-*co*-εCL)-*b*-PEG-*b*-poly(αN3εCL-*co*-εCL) copolymers (CP5, CP6, and CP7). Characteristics of all copolymers are summarized in **Table 2**.

Table 2. Characteristics of poly(αN3εCL-*co*-εCL)-*b*-PEG-*b*-poly(αN3εCL-*co*-εCL) copolymers prepared by nucleophilic substitution[a]

Copolymer	$f_{\alpha N_3\varepsilon CL}$[b]	$F_{\alpha N_3\varepsilon CL}$[c]	Yield (%)	$M_{n,th}$[d] (g.mol^{-1})	$M_{n,NMR}$[e] (g.mol^{-1})	$M_{n,SEC}$[f] (g.mol^{-1})	$Đ$[f]
CP5	0.09	0.08	90	3400	3300	5300	1.39
CP6	0.23	0.21	96	3500	3400	5500	1.50
CP7	0.47	0.44	94	3700	3800	5400	1.41

[a] Conditions: NaN_3 (10 eq. / αClεCL unit), solvent: DMF, room temperature, time = 24 hours; [b] $f_{\alpha N3\varepsilon CL} = F_{\alpha Cl\varepsilon CL}$; [c] calculated from **Equation 3**; [d] $M_{n,th} = M_{n,PEG} + [(([\alpha N_3\varepsilon CL]_0/[PEG]_0) \times 155) + (([\varepsilon CL]_0/[PEG]_0) \times 114)]$; [e] calculated from **Equation 4**; [f] determined by SEC in THF using polystyrene standards.

The presence of azido groups on the PεCL backbone was evidenced by infrared spectroscopy (**Figure 2**) with the presence of the characteristic band of the azide function at 2100 cm^{-1}. Additionally, it is important to notice that a clear increase of this band was observed with the molar ratio in αN3εCL monomeric unit when spectra were normalized with band at 1740 cm^{-1}, which corresponded to vibration of the carbonyl bond.

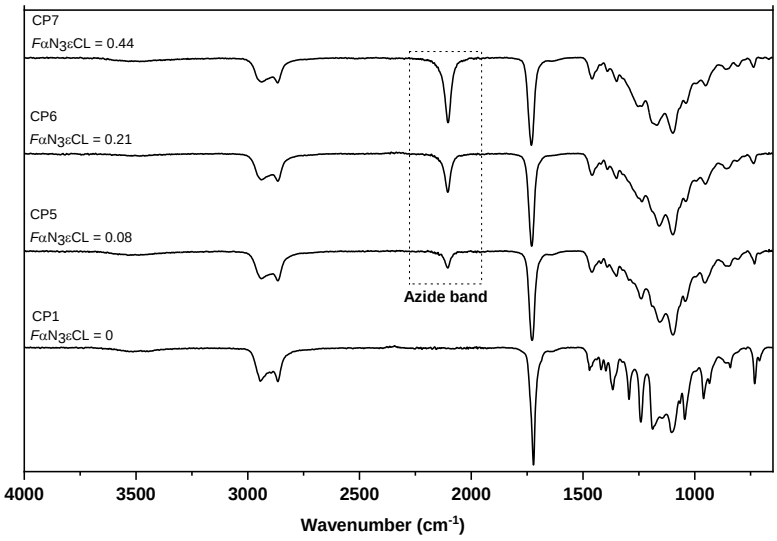

Figure 2. FTIR spectra of poly(εCL)-*b*-PEG-*b*-poly(εCL), namely CP1, $F_{\alpha N3\varepsilon CL}$ = 0, and poly(αN$_3$εCL-*co*-εCL)-*b*-PEG-*b*-poly(αN$_3$εCL-*co*-εCL), namely CP2, CP3, CP4 with $F_{\alpha N3\varepsilon CL}$ = 0.08, 0.21, 0.44, respectively.

The presence of the azide function was confirmed by ^{1}H NMR spectroscopy (**Figure 3** and **Figure S4**). Indeed, a new peak at δ 3.80 ppm (peak A) (**Figure 3**) was assigned to the methine in the α-position of azide group borne by the αN$_3$εCL monomeric unit. We can also mention the disappearance of the signal corresponding to the proton in the α-position of the chlorine atom at 4.26 ppm.

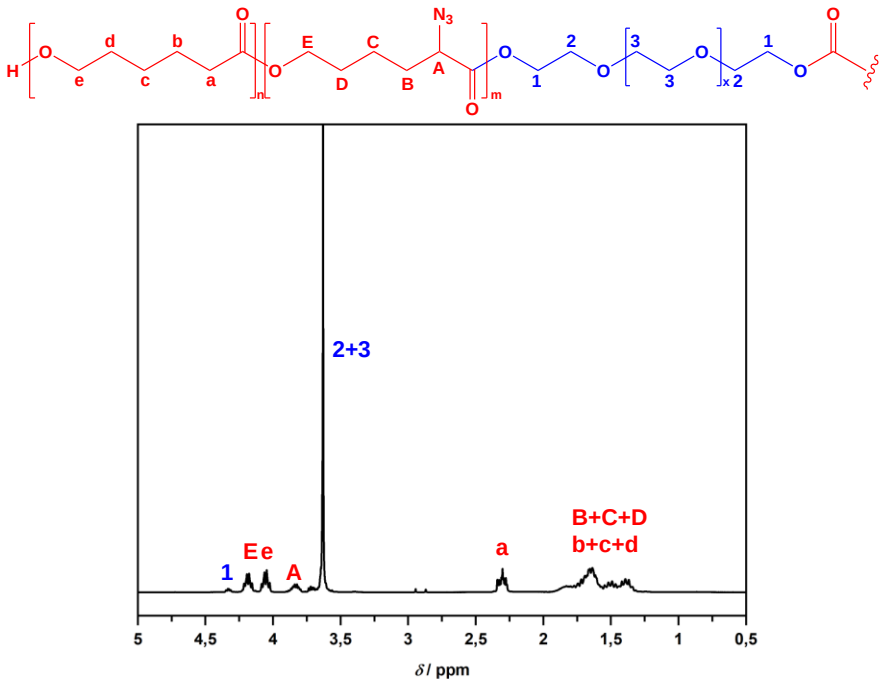

Figure 3. ^{1}H NMR spectrum in deuterated chloroform of poly(αN$_3$εCL-*co*-εCL)-*b*-PEG-*b*-poly(αN$_3$εCL-*co*-εCL) (CP7); $F_{\alpha N3\varepsilon CL}$ = 0.44.

Characterization analyses confirmed the almost quantitative conversion of the pendent chlorine due to the high efficiency of the nucleophilic substitution. Indeed, experimental molar ratios of αN$_3$εCL ($F_{\alpha N3\varepsilon CL}$) were close from theoretical ones ($f_{\alpha N3\varepsilon CL}$). Additionally, the experimental molar masses determined by ^{1}H NMR were very similar from theoretical ones. SEC traces were monomodal (**Figure S5**), with no significant changes of the molecular weights and the dispersities (*Đ*) in comparison with starting poly(αClεCL-*co*-εCL)-*b*-PEG-*b*-poly(αClεCL-*co*-εCL) materials. Those results allowed us to conclude that the conversion of the halogen atom was efficient, with no degradation of the polyester backbone.

Synthesis of poly(αTzBPεCL-*co*-εCL)-*b*-PEG-*b*-poly(αTzBPεCL-*co*-εCL). In a last step, functional copolymers based on PεCL and PEG bearing pendent aminobisphosphonate complexing moieties were prepared *via* Huisgen 1,3-dipolar cycloaddition (**Scheme 1**). The azide-functionalized copolymers were coupled with an acetylenic aminobisphosphonate in the presence of copper (I) bromide/pentamethyldiethylenetriamine (CuBr/PMDETA) complex as catalytic system in DMF at room temperature for 24 hours. A slight excess of α-aminobisphosphonate (1.1 equiv.) was used in order to enhance the grafting efficiency. The crude materials were purified by precipitation in diethyl ether in order to remove unreacted bisphosphonate. Experimental results of these functional copolymers are summarized in **Table 3**.

Table 3. Characteristics of poly(αTzBPεCL-*co*-εCL)-*b*-PEG-*b*-poly(αTzBPεCL-*co*-εCL) synthesized[a]

Copolymer	$f_{\alpha TzBP\varepsilon CL}$ [b]	$F_{\alpha TzBP\varepsilon CL}$ [c]	Yield (%)	$M_{n,th}$ [d] ($g.mol^{-1}$)	$M_{n,NMR}$ [e] ($g.mol^{-1}$)	$M_{n,SEC}$ [f] ($g.mol^{-1}$)	$Đ$ [f]
CP8	0.08	0.07	40	4000	4800	7300	1.41
CP9	0.21	0.18	63	5000	5300	-	-
CP10	0.44	0.38	52	6700	6400	-	-

[a] Conditions: CuBr/PMDETA=1/2, solvent: DMF, room temperature, time = 24 hours; [b] $f_{\alpha TzBP\varepsilon CL} = F_{\alpha N3\varepsilon CL}$; [c] calculated from **Equation 5**; [d] $M_{n,th} = M_{n,PEG} + [(([\alpha TzBP\varepsilon CL]_0/[PEG]_0) \times 454) + (([\varepsilon CL]_0/[PEG]_0) \times 114)]$; [e] calculated from **Equation 6**; [f] determined by SEC in THF using polystyrene standards.

Functionalized copolymers were notably characterized by ^{1}H NMR (**Figure 4**), which allowed proving the incorporation of the complexing moiety with new signals at δ 3.10 and 3.70 ppm assigned to the protons of the α-aminobisphosphonate ligand. A shift of the peak from δ 3.80 ppm to δ 5.25 ppm (peak A) was observed related to the methine proton of -COC*H*triazole-group of the αTzBPεCL monomeric unit. Additionally, the signal at δ 7.80 ppm was attributed to

the proton of the triazole ring. These different peaks evidenced the grafting of the bisphosphonate to the PεCL backbone. Grafting efficiency was also calculated according to Equation 6 comparing signals at δ 3.71 ppm for αTzBP$_3$εCL unit and at δ 2.30 ppm for εCL. Experimental values were close from theoretical ones ($f_{\alpha TzBP\varepsilon CL}$ = 0.08, 0.21, and 0.44), with $F_{\alpha TzBP\varepsilon CL}$ equal to 0.07, 0.18, and 0.38, for CP8, CP9, and CP10, respectively. An overlay of the ^{1}H NMR spectra of the non-functionalized copolymer (CP1) and the three α-aminobisphosphonate-based copolymers (CP8, CP9 and CP10) (**Figure S6**) showed an increase of the intensities of the signals at δ 3.10 and 3.70 ppm with the increase of the ligand experimental molar ratio. ^{31}P NMR spectrum (**Figure 4 inset**) confirmed the successful grafting of the bisphosphonate onto the copolymers with the presence of a single peak at δ 26.46 ppm, thus demonstrating the presence of a single phosphorus population within the polymer.

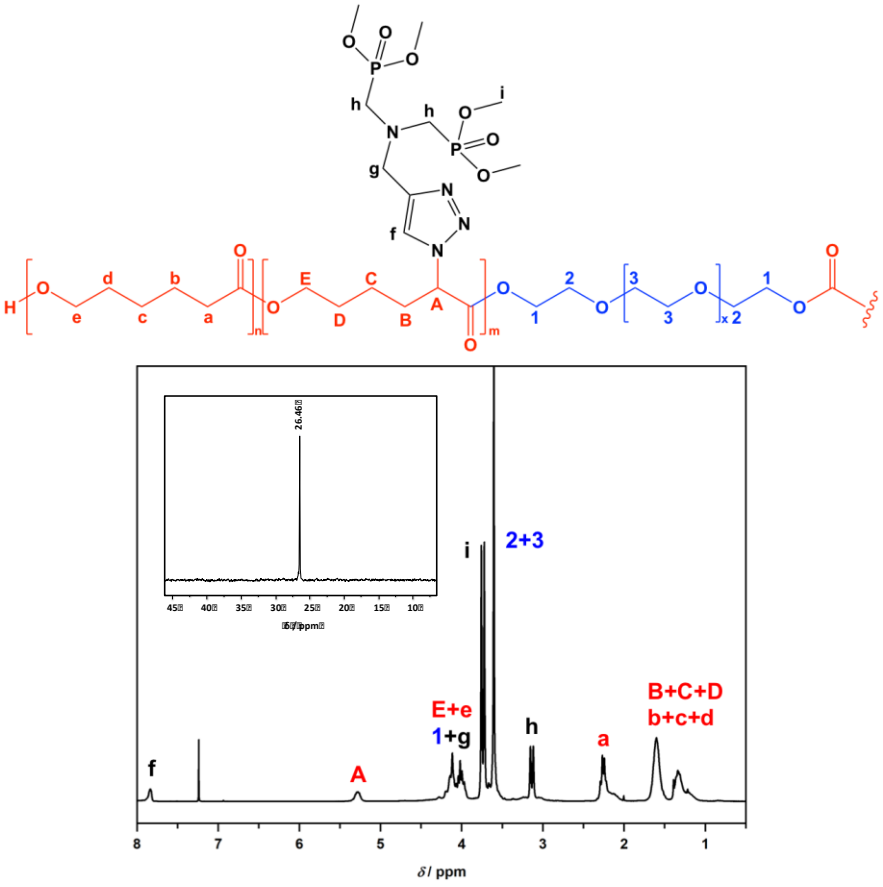

Figure 4. ^{1}H NMR spectrum (and ^{31}P NMR spectrum in inset) in deuterated chloroform of poly(αTzBPεCL-*co*-εCL)-*b*-PEG-*b*-poly(αTzBPεCL-*co*-εCL) (CP10); $F_{\alpha TzBP\varepsilon CL}$ = 0.38.

The molecular weights ($M_{n,NMR}$) of final copolymers were calculated from the relative intensity of the ^{1}H NMR signals of both ε-caprolactone units and the ethylene glycol monomeric units (**Equation 6**). The experimental values were close from theoretical ones. Finally, SEC trace showed a shift toward higher molecular weight in comparison with the azido-functionalized copolymers providing an additional evidence of the grafting. In particular, CP8 SEC trace ($F_{\alpha TzBP\varepsilon CL}$ = 0.07) (**Figure 5**) clearly shifted to higher molecular weight in comparison with

chromatogram corresponding to CP5 azido-based copolymer, without chain degradation. In particular, polyester backbone did not undergo degradation as we worked under mild conditions at room temperature, which already proved to lead to efficient click chemistry reactions without side reactions.[38-40] Finally, it is important to notice that SEC analyses could not be performed for CP9 ($F_{\alpha TzBP\varepsilon CL}$ = 0.18) and CP10 ($F_{\alpha TzBP\varepsilon CL}$ = 0.38) copolymers due to their poor solubility in THF or DMF.

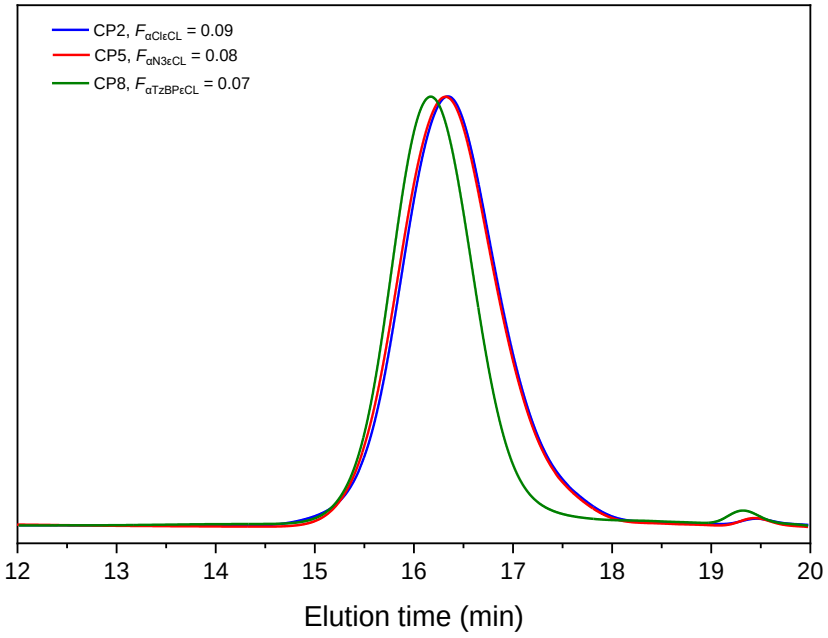

Figure 5. Size exclusion chromatograms of poly(αClεCL-*co*-εCL)-*b*-PEG-*b*-poly(αClεCL-*co*-εCL) CP2 (blue), poly(αN_3εCL-*co*-εCL)-*b*-PEG-*b*-poly(αN_3CL-*co*-εCL) CP5 (red), and poly(αTzBPεCL-*co*-εCL)-*b*-PEG-*b*-poly(αTzBPεCL-*co*-εCL) CP8 (green).

To conclude, click process was efficient, with an almost quantitative conversion of azide species to bisphosphonate moieties. All experimental results proved the successful synthesis of well-defined polyesters having different ratios of complexing α-aminobisphosphonate ligand. Afterwards, the three synthesized copolymers with different bisphosphonate ligand molar ratios

(7, 18, and 38 %) were evaluated for the sorption properties (constant and stoichiometry) of two lanthanides (neptunium and cerium) used as actinide surrogates.

Complexation studies by Isothermal Titration Calorimetry (ITC). Complexing properties of the three CP8, CP9, and CP10 copolymers with neodymium and cerium were analyzed by Isothermal Titration Calorimetry (ITC). These two elements were chosen, as they are surrogates of uranium and plutonium, respectively, thus showing the same properties and as a result the same characteristics in terms of binding constant and stochiometry. In order to determine the ionic species present in solution at the pH chosen for the experiments, preliminary speciation diagrams have been established. Thus, at pH 5.5 (specifically chosen as it corresponded to the pH of the skin) the tested lanthanides were soluble in water and available as cations. **Figure 6** shows the thermogram of the system CP9 copolymer ($F_{\alpha TzBP\varepsilon CL}$ = 0.18)/Nd(III), superposed at the dilution in Milli-Q water at 25 °C and pH 5.5 (top), as well as the ITC titration curve obtained for the polymer (bottom).

On the thermogram of the copolymer-Nd(III) system (in black), the signals characteristics of the interaction between the ligand and the cation were endothermic and the first peak showed a heat rate equal to -0.85 µW. Thereafter, the intensity increased until the inversion of signal after nearly 7 injections. Finally, the signal seemed stabilized at around 0.25-0.30 µW for the last 10-12 injections. In comparison, the dilution thermogram (in grey) showed only exothermic signals with an intensity of about 0.35-0.40 µW. Thus, the steady state observed for the copolymer-Nd(III) system was similar to the dilution. This meant that only the dilution effects were still detected. In other words, no more interactions between the polymer and Nd(III) occurred. So, the complexation did not take place anymore, and therefore all available chelating sites seemed to be

saturated or not accessible. The difference between both thermograms clearly showed that an interaction occurred between the copolymer and Nd(III). In order to confirm the role of the bisphosphonate moieties in the complexation of cations, ITC tests with the unfunctionalized polymer (CP1) and Nd(III) were performed. The thermogram obtained was identical to that of the dilution alone, showing the absence of interactions between the polymer and Nd(III). Thus, these results confirmed the effectiveness of the bisphosphonate groups in complexation.

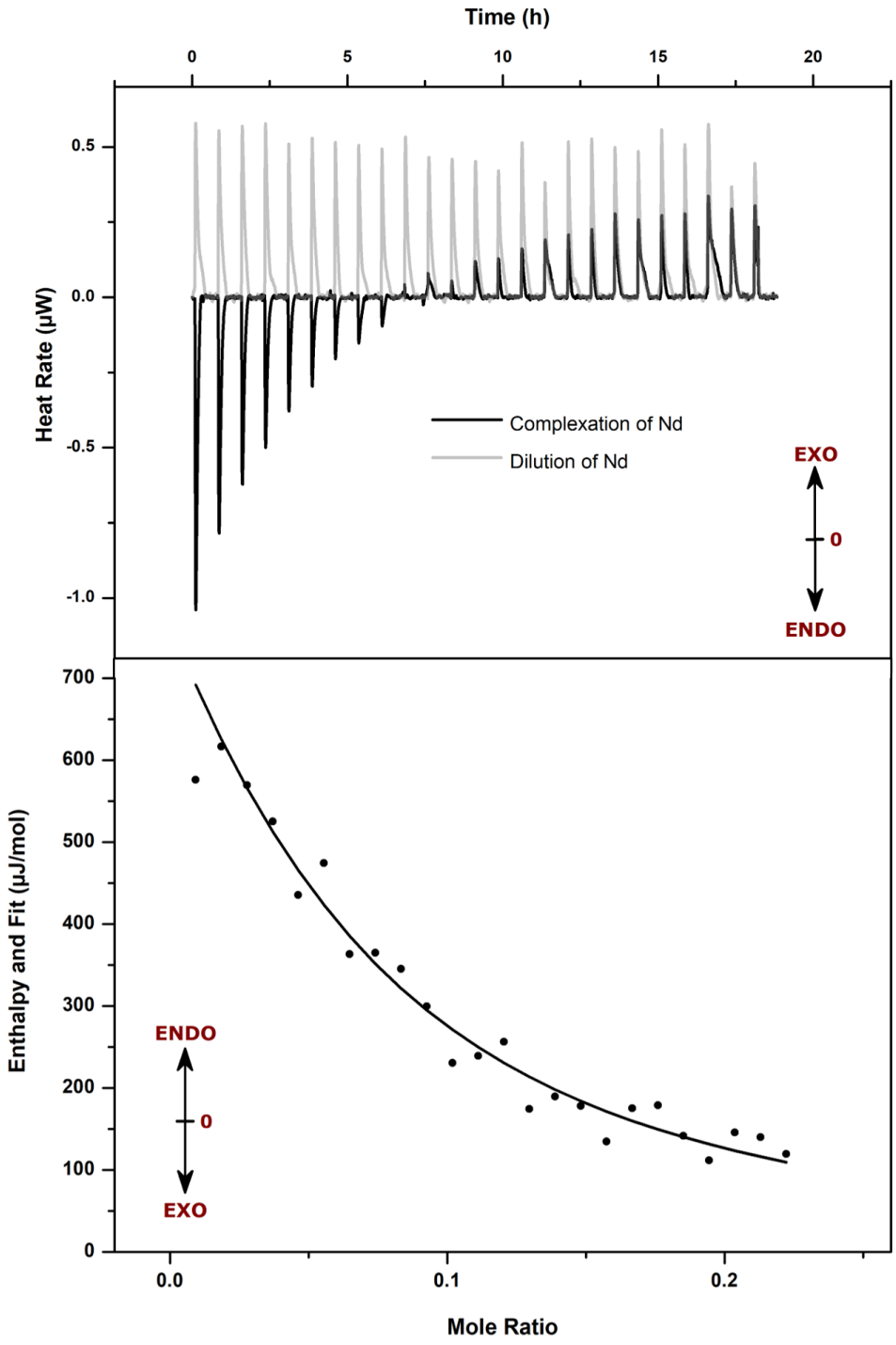

Figure 6. ITC thermogram (top) and titration curve (bottom) of CP9 (1.3 $g.L^{-1}$) (*F*αTzBPεCL = 0.18) with Nd(III) (3 mM).

The titration curve was obtained by integrating the peaks of the thermogram for each injection and by plotting the curve fitting of these integrations (heat flow) as a function of the mole ratio of functional groups, using one set of site-binding model. This curve allowed obtaining the thermodynamic constants of the studied system, in particular the reaction constants and the stoichiometry (n) which gave information on the number of ligands necessary to complex one cation. Thus, for the CP9 copolymer, the stoichiometry (number of moles of cation divided by the number of moles of ligand) obtained was 0.22, meaning that 4-5 ligands could complex one Nd(III) cation. Meanwhile, the same experiments were carried out with the copolymers containing 7 and 38 % of bisphosphonate functions (CP8, and CP10, respectively) to compare their complexation efficiency according to their degree of functionalization (**Figure S7-S11**). The thermodynamic constants obtained with the fits of the titration curves of these three copolymers are summarized in **Figure 7**. The first figure (top left) shows the inverse of the stoichiometry, *i.e.* the number of bisphosphonate functions necessary to complex one cation, according to the different polymers and cations tested. For a given cation, the amount of ligand per metal ion decreased when the number of bisphosphonate functions increased (CP8 > CP9 > CP10), meaning that for the same number of functions, the structure of CP10 made its functional group accessible and was able to complex a larger quantity of cations. In addition, this number of ligands required for the complexation of one cation was higher with Ce(III) than with Nd(III), showing that these copolymers complexed Nd(III) better than Ce(III). The **Figure 7** (top right) represents the binding constant between the copolymers (or the ligands in the copolymers) and the ions tested. The constants were in the range of 10^3 - 2.5 10^4 M^{-1}. Generally speaking, binding constants for sorption (complexation, exchange, adsorption) are in the range of 10^{+8} M^{-1} or even higher for strong interaction such as for metal ions binding to peptides.[41] In the case of

low-cost sorbents (biopolymer, clays, zeolites, etc.) the affinity is lower, with relative weak binding sites.[42] Our results were in the range of average value for the complexation. For both cations, these constants were higher for the copolymer containing the fewest bisphosphonate complexing functions (CP8). In addition, they were slightly higher with Nd(III) than with Ce(III), but values remained very close. Thus, if the CP10 copolymer exhibited a higher stoichiometry than the CP8, and thus extracted more cation, its bonds formed with the cations were a lot weaker. CP9, on the other hand, was an intermediate with slightly lower stoichiometry than CP10 but greater binding constants, making it attractive for the final application of actinides retention and possible body decontamination. Finally, **Figure 7** on the bottom shows the entropy (ΔS), enthalpy (ΔH) and Gibbs free energy (ΔG) variation constants for each functionalized copolymer, according to the cations tested. These data demonstrated that for the three polymers, the system was entropically driven, whatever the cation tested, like many systems used for the complexation of cations. Indeed, diethylenetriaminepentaacetic acid (DTPA), usually used for the complexation of actinides, was also an entropic system,[43] as well as other systems based on functionalized polymers.[44-46] This could be explained by several mechanisms generally involved in such phenomena, with the release of counterions, the modification of hydration sphere of ions, and the loss of water molecules, as well as by the decrease of long-range solvent ordering during the binding process.

Additionally, the ΔG variation of our systems was between -20 and -30 $kJ.mol^{-1}$, showing that the complexation of cations was a favorable and spontaneous reaction. In comparison, another system described in the literature containing phosphonated ester type complexing groups for the

complexation of Ce(III) showed a much higher ΔG (-2.12 kJ.mol^{-1}),[47] proving that this system was less favorable for the extraction of this cation than our systems.

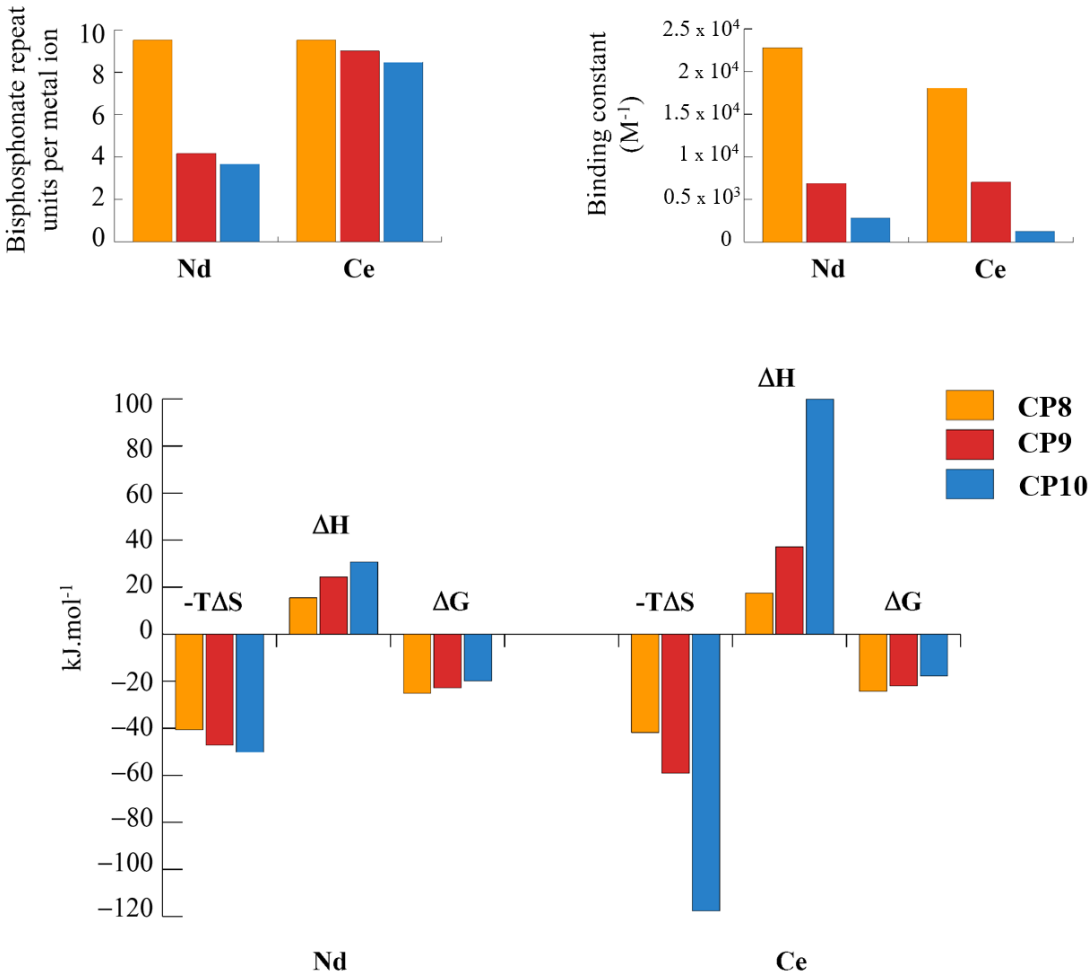

Figure 7. On the top corner left, stoichiometry of metal ions binding for the three copolymers functionalized; on the top corner right, binding constants of the three copolymers with the metal ions; on the bottom, thermodynamic constants of Nd(III) and Ce(III) binding to the three copolymers (CP8, CP9, and CP10).

In order to investigate the possible use of the synthesized copolymers for actinide complexation, the maximum sorption capacities (q_{max}) of the three CP8, CP9, and CP10

copolymers studied with Nd(III) and Ce(III) cations were calculated from the obtained stoichiometry and compared with those in the literature for systems used for the complexation, adsorption or exchange of Nd(III) or Ce(III) (**Table 4** and **Table 5**). It is important to mention that a preliminary study varying the pH from 2 to 9 allowed us to determine that the pH leading to the highest sorption efficiencies was equal to 5-6. As a consequence, experiments were achieved at pH = 5.5.

Table 4. Comparison of sorption efficiencies of different sorbents for Nd(III) ions

Sorbent	pH	Sorption capacity ($mg.g^{-1}$)	Reference
Transcarpathian clinoptilolite (Zeolite)	6.5	1.81	[48]
Carbonized parachlorella 250 °C	7	5.53	[49]
Impregnated SiO_2/UF composite	3	4.959	[50]
Cyphos@silica	4	13.4	[51]
Silica gel modified with diglycol amic acid	1	16.15	[52]
Chitosan/Iron(III) hydroxide	4	13.8	[53]
Chitosan-based material	5	30.32	[54]
Microorganisms	1.5	10-12	[55]
Magnetic nano-hydroxyapatite	5.5	323	[56]
CP8 ($F_{\alpha TzBP\varepsilon CL}$ = 0.07)	5.5	4.3	this work
CP9 ($F_{\alpha TzBP\varepsilon CL}$ = 0.18)	5.5	21.4	this work
CP10 ($F_{\alpha TzBP\varepsilon CL}$ = 0.38)	5.5	34.0	this work

Thus, the CP8, CP9 and CP10 copolymers had sorption capacities equal to 4.3, 21.4 and 34.0 $mg.g^{-1}$ for Nd(III), and 4.1, 9.6, 14.3 $mg.g^{-1}$ for Ce(III), respectively. This meant that for example, 34.0 mg of Nd(III) could be adsorbed per gram of CP10 copolymer. Thus, by increasing the quantity of bisphosphonate functions, the maximum sorption capacity also increased, making the CP10 copolymer very attractive for the complexation and the removal of

Nd(III) and Ce(III) ions. In addition, for the sorption of Nd(III), the CP9 and CP10 copolymers had a higher q_{max} than most of the materials used to complex neodymium. Indeed, in **Table 4**, only the chitosan-based material,[54] and the magnetic nano-hydroxyapatite[56] had a higher sorption capacity than our two polymers, and this great difference in sorption could be explained by different sorption mechanisms. Indeed, magnetic nano-hydroxyapatites are inorganic solid particles, ion exchange and adsorption more commonly occurred in such materials. On the other hand, these polymers were less efficient for Ce(III) sorption because even the highest capacity (for CP10) remained lower than many systems described in the literature. However, when compared with the sorption capacity already reported and obtained specifically for polymer (2.48 $mg.g^{-1}$),[57] those obtained for CP8, CP9 and CP10 α-aminobisphosphonate-based copolymers were higher.

Table 5. Comparison of sorption efficiencies of different sorbents for Ce(III) ion

Sorbent	pH	Sorption capacity ($mg.g^{-1}$)	Reference
TPDP ligand / mesoporous silica monoliths	3.5	192.31	[58]
MnOH	5.5	45.5	[59]
MnO_2	5.5	22.2	[59]
Mn_3O_4	5.5	7.7	[59]
Spirulina biomass	5.5	18.1	[60]
Polymer supported o-vanillinsemicarbazone	6-9	2.48	[57]
Platanus orientalis leaf powder	4	32.05	[61]
CP8 ($F_{\alpha TzBP\varepsilon CL}$ = 0.07)	5.5	4.1	this work
CP9 ($F_{\alpha TzBP\varepsilon CL}$ = 0.18)	5.5	9.6	this work
CP10 ($F_{\alpha TzBP\varepsilon CL}$ = 0.38)	5.5	14.3	this work

CONCLUSIONS

This paper reports the synthesis and the evaluation of sorption properties for neodymium and cerium (surrogates of uranium and plutonium, respectively) of original copolymers composed of poly(ethylene glycol) and poly(ε-caprolactone) bearing pendent α-aminobisphosphonate moieties. Three copolymers with different α-aminobisphosphonate molar ratios were synthesized to study the influence of the amount of this moiety on the complexation capacities of the copolymers. The synthesis was based on the copolymerization of ε-caprolactone and α-chloro-ε-caprolactone using poly(ethylene glycol) as macro-initiator, followed by chemical modification to convert the pendent chloride groups into azido groups. Finally, the grafting of the aminobisphosphonate ligand was achieved using click chemistry. The resulting copolymers were characterized by ^{1}H and ^{31}P NMR, which confirmed the synthesis of the poly(αTzBPεCL-*co*-εCL)-*b*-PEG-*b*-poly(αTzBPεCL-*co*-εCL) with functionalization ratios equal to 7, 18 and 38 %, proving that azide species were successfully converted to α-aminobisphosphonate moieties. Additionally, ^{1}H NMR and size exclusion chromatography measurements allowed the determination of the copolymer molecular weights and dispersities, which were around 3500 $g.mol^{-1}$ and 1.40-1.50, respectively.

Then, sorption capacities of the three synthesized valuable copolymers toward two lanthanides, Nd(III) and Ce(III), used as actinide surrogates, were evaluated using Isothermal Titration Calorimetry to determine the stoichiometry and the reaction constant. The results showed the efficiency of the α-aminobisphosphonate function for the complexation of both Nd(III) and Ce(III) ions at pH 5.5, in particular for CP9 and CP10. Indeed, the latter had the greatest stoichiometry of binding as well as the highest sorption capacity, making it more efficient than

most of the materials already described in the literature for the complexation of neodymium and cerium. However, its binding constant was the lowest. CP9 could be a good alternative because its stoichiometry and q_{max} were high and its constant binding was great, making it efficient for the extraction of ions. In particular, these new valuable copolymers could be successfully employed in the field of body decontamination to treat contaminated skin, where the pH value proved to be around 5.5. The use of these polymeric materials, based on non-toxic and biocompatible segments, would avoid diffusion through the skin barrier, thus avoiding additional contamination after complexation, and leading to an efficient decontamination. To conclude, the developed copolymers represent a very valuable opportunity in a domain where commercial solutions are nowadays still very limited.

ASSOCIATED CONTENT

Supporting Information

The Supporting Information is available free of charge at https://pubs.acs.org/doi/xx.xxxx/acs.biomac.xxxxxxx.

^{1}H NMR spectra of monomer and polymers, size exclusion chromatograms of polymers, ITC thermographs (PDF).

AUTHOR INFORMATION

Corresponding Authors

* Vincent Darcos - IBMM, Univ Montpellier, CNRS, ENSCM, Montpellier, France; Email: vincent.darcos@umontpellier.fr; * Sophie Monge - ICGM, Univ Montpellier, CNRS, ENSCM, Monptellier, France; Email: sophie.monge-darcos@umontpellier.fr

Authors

Carlos Arrambide - IBMM, Univ Montpellier, CNRS, ENSCM, Montpellier, France; Loona Ferrie - ICGM, Univ Montpellier, CNRS, ENSCM, Montpellier, France; Benedicte Prelot - ICGM, Univ Montpellier, CNRS, ENSCM, Montpellier, France; Amine Geneste - ICGM, Univ Montpellier, CNRS, ENSCM, Montpellier, France

Author Contributions

The manuscript was written through contributions of all authors. All authors have given approval to the final version of the manuscript.

Note

The authors declare no competing financial interest.

Funding Source

ANR DECAP (ANR-18-ASTR-0001) (CA); “Agence Innovation Défense” (AID) (LF)

ACKNOWLEDGEMENTS

The authors thank “Agence Innovation Défense” (AID) (PhD grant (LF)), and ANR DECAP (ANR-18-ASTR-0001) (CA)) for funding this work. They also thank the “Plateforme d’Analyses et de Caractérisation” (PAC Balard) for technical support in analysis and characterizations, and the SynBio3 platform for SEC analyses.

REFERENCES

1. Cheng, E. T., Performance characteristics of actinide-burning fusion power plants. *Fusion Sci. Technol.* **2005,** *47* (4), 1219-1223.

2. Choppin, G., Actinide chemistry: from weapons to remediation to stewardship. *Radiochim. Acta* **2004,** *92* (9-11), 519-523.

3. Hare, S. S.; Goddard, I.; Ward, P.; Naraghi, A.; Dick, E. A., The radiological management of bomb blast injury. *Clin. Radiol.* **2007,** *62* (1), 1-9.

4. Cherry, S.; Sorenson, J.; Phelps, M., Physics in Nuclear Medicine E-Book, Elsevier Health Science **2012**.

5. Van Leeuwen, P. J.; Emmett, L.; Ho, B.; Delprado, W.; Ting, F.; Nguyen, Q.; Stricker, P. D., Prospective evaluation of ^{68}Gallium-prostate-specific membrane antigen positron emission tomography/computed tomography for preoperative lymph node staging in prostate cancer. *Bju Int.* **2017,** *119* (2), 209-215.

6. Soule, S.; Kouakam, C., This is the end. *Arch. Cardiovasc. Dis. Suppl.* **2018,** *10* (1), 100-101.

7. Grappin, L.; Berard, P.; Menetrier, F.; Carbone, L.; Courtay, C.; Castagnet, X.; Le Goff, J. P.; Neron, M. O.; Piechowski, J., Treatment of actinide exposures: A review of Ca-DTPA injections inside CEA-COGEMA plants. *Radiat. Prot. Dosim.* **2007,** *127* (1-4), 435-439.

8. Bleise, A.; Danesi, P. R.; Burkart, W., Properties, use and health effects of depleted uranium (DU): a general overview. *J. Environ. Radioact.* **2003,** *64* (2-3), 93-112.

9. Durakovic, A., Medical effects of internal contamination with actinides: further controversy on depleted uranium and radioactive warfare. *Environ. Health Prev. Med.* **2016,** *21* (3), 111-117.

10. Younes, A.; Creff, G.; Beccia, M. R.; Moisy, P.; Roques, J.; Aupiais, J.; Henning, C.; Solari, P. L.; Den Auwer, C.; Vidaud, C., Is hydroxypyridonate 3,4,3-Li(1,2-HOPO) a good competitor of fetuin for uranyl metabolism? *Metallomics* **2019,** *11* (2), 496-507.

11. Zhang, Q.; Jin, B.; Zheng, T.; Tang, X.; Guo, Z.; Peng, R., Hexadentate β-Dicarbonyl(bis-catecholamine) Ligands for Efficient Uranyl Cation Decorporation: Thermodynamic and Antioxidant Activity Studies. *Inorg. Chem.* **2019,** *58*, 14626-14634.

12. Chen, B.; Hong, S.; Dai, X.; Li, X.; Huang, Q.; Sun, T.; Cao, D.; Zhang, H.; Chai, Z.; Diwu, J.; Wang, S., In vivo uranium decorporation by a tailor-made hexadentate ligand. *J. Am. Chem. Soc.* **2022,** *144* (25), 11054-11058.

13. Fattal, E.; Tsapis, N.; Phan, G., Novel drug delivery systems for actinides (uranium and plutonium) decontamination agents. *Adv. Drug Deliv. Rev.* **2015,** *90*, 40-54.

14. Yantasee, W.; Sangvanich, T.; Creim, A.; Pattamakomsan, K.; Wiacek, R. J.; Fryxell, G. E.; Addleman, R. S.; Timchalk, C., Functional sorbents for selective capture of plutonium, americium, uranium, and thorium in blood. *Health Phys.* **2010,** *99* (3), 413-419.

15. James, A. C.; Sasser, L. B.; Stuit, D. B.; Glover, S. E.; Carbaugh, E. H., Ustur whole body case 0269: demonstrating effectiveness of i.v. Ca-DTPA dor Pu. *Radiat. Prot. Dosim* **2007,** *127* (1-4), 449-455.

16. Durbin, P. W.; Kullgren, B.; Schmidt, C. T., Circulatory kinetics of intravenously injected Pu-238(IV) citrate and C-14-CaNa3-DTPA in mice: Comparison with rat, dog, and reference man. *Health Phys.* **1997,** *72* (2), 222-235.

17. Grives, S.; Phan, G.; C., B.-C.; Suhard, D.; Rebiere, F.; Agarande, M.; Fattal, E., Compared in vivo efficiency of nanoemulsions unloaded and loaded with calixarene and soapy

water in the treatment of superficial wounds contaminated by uranium. *Chem. Biol. Interact.* **2017,** *267*, 33-39.

18. Belhomme-Henry, C.; Phan, G.; Huang, N.; Bouvier, C.; Rebiere, F.; Agarande, M.; Fattal, E., Texturing formulations for uranium skin decontamination. *Pharm. Dev. Technol.* **2014,** *19* (6), 692-701.

19. Grives, S.; Phan, G.; Morat, G.; Suhard, D.; Rebiere, F.; Fattal, E., Ex vivo uranium decontamination efficiency on wounded skin and in vitro skin toxicity of a calixarene-loaded nanoemulsion. *J. Pharm. Sci.* **2015,** *104*, 2008-2015.

20. Bollinger, J. E.; Roundhill, D. M., Complexation of the uranyl ion with the aminomethylenediphosphonates MAMDP and AMDP. *Inorg. Chem.* **1994,** *33*, 6421-6424.

21. Henge-Napoli, M. H.; Ansoborlo, E.; Chazel, V.; Houpert, P.; Paquet, F.; Gourmelon, P., Efficacy of ethane-1-hydroxy-1,1-bisphosphonate (EHBP) for the decorporation of uranium after intramuscular contamination in rats. *Int. J. Radiat. Biol.* **1999,** *75* (11), 1473-1477.

22. Fukuda, S.; Iida, H.; Ikeda, M.; Yan, X. M.; Xie, Y. Y., Toxicity of uranium and the removal effects of CBMIDA and EHBP in simulated wounds of rats. *Health Phys.* **2005,** *89* (1), 81-88.

23. Chaleix, V.; Lecouvey, M., Synthesis of novel phosphonated tritpodal ligands for actinides chelation therapy. *Tetrahedron Lett.* **2007,** *48* (4), 703-706.

24. Ansoborlo, E.; Amekraz, B.; Moulin, C.; Moulin, V.; Taran, F.; Bailly, T.; Burgada, R.; Henge-Napoli, M. H.; Jeanson, A.; Den Auwer, C.; Moisy, P., *C. R. Chimie* **2007,** *10*, 1010-1019.

25. Migianu-Griffoni, E.; Mbemba, C.; Burgada, R.; Lecercle, D.; Taran, F.; Lecouvey, M., Design and synthesis of new polyphosphorylated upper-rim modified calix[4]arenes as potential and selective chelating agents of uranyl ion. *Tetrahedron* **2009,** *65* (65), 1517-1523.

26. Wang, L.; Yang, Z.; Gao, J.; Xu, K.; Gu, H.; Zhang, B.; Zhang, X.; Xu, B., A Biocompatible method of decorporation: bisphosphonate-modified magnetite nanoparticles to remove uranyl ions from blood. *J. Am. Chem. Soc.* **2006,** *128* (41), 13358-13359.

27. Wang, X. M.; Shi, C.; Guan, J. W.; Chen, Y. M.; Xu, Y. G.; Diwu, J.; Wang, S., The development of molecular and nano actinide decorporation agents. *Chin. Chem. Lett.* **2022,** *33* (7), 3395-3404.

28. D'Souza, A. A.; Shegokar, R., Polyethylene glycol (PEG): a versatile polymer for pharmaceutical applications. *Expert Opin. Drug Deliv.* **2016,** *13* (9), 1257-1275.

29. Al Samad, A.; Bethry, A.; Koziolova, E.; Netopilik, M.; Etrych, T.; Bakkour, Y.; Coudane, J.; El Omar, F.; Nottelet, B., PCL-PEG graft copolymers with tunable amphiphilicity as efficient drug delivery systems. *J. Mater. Chem. B* **2016,** *4* (37), 6228-6239.

30. Singh, S.; Alrobaian, M. M.; Molugulu, N.; Agrawal, N.; Numan, A.; Kesharwani, P., Pyramid-shaped PEG-PCL-PEG polymeric-based model systems for site-specific drug delivery of vancomycin with enhance antibacterial efficacy. *ACS Omega* **2020,** *5* (21), 11935-11945.

31. Deng, H. Z.; Dong, A. J.; Song, J. B.; Chen, X. Y., Injectable thermosensitive hydrogel systems based on functional PEG/PCL block polymer for local drug delivery. *J Controlled Release* **2019,** *297*, 60-70.

32. Mondal, P.; Behera, P. K.; Singha, N. K., Macromolecular engineering in functional polymers via 'click chemistry' using triazolinedione derivatives. *Prog. Polym. Sci.* **2021,** *113,* 101343.

33. Tremblay-Parrado, K. K.; Garcia-Astrain, C.; Averous, L., Click chemistry for the synthesis of biobased polymers and networks derived from vegetable oils. *Green Chem.* **2021,** *23* (12), 4296-4327.

34. Kaur, J.; Saxena, M.; Rishi, N., An Overview of Recent Advances in Biomedical Applications of Click Chemistry. *Bioconjug. Chem.* **2021,** *32* (8), 1455-1471.

35. Ferrie, L.; Arrambide, C.; Darcos, V.; Prelot, B.; Monge, S., Synthesis and evaluation of functional carboxylic acid based poly (epsilon CL-st-alpha COOH epsilon CL)-b-PEG-b-poly(epsilon CL-st-alpha COOH epsilon CL) copolymers for neodymium and cerium complexation. *React. Funct. Polym.* **2022,** *171*, 105157.

36. Lenoir, S.; Riva, R.; Lou, X.; Detrembleur, C.; Jerome, R.; Lecomte, P., Ring-opening polymerization of α-chloro-ε-caprolactone and chemical modification of poly(α-chloro-ε-caprolactone) by atom transfer radical processes. *Macromolecules* **2004,** *37* (11), 4055-4061.

37. Cavero, E.; Zablocka, M.; Caminade, A.-M.; Majoral, J. P., Design of bisphosphonate-terminated dendrimers. *EurJOC* **2010,** *2010* (14), 2759-2767.

38. Darcos, V.; El Habnouni, S.; Nottelet, B.; El Ghzaoui, A.; Coudane, J., Well-defined PCL-graft-PDMAEMA prepared by ring-opening polymerization and click chemistry. *Polym. Chem.* **2010,** *1*, 280-282.

39. Darcos, V.; Al Tabchi, H.; Coudane, J., Synthesis of PCL-graft-PS by combination of ROP, ATRP, and click chemistry. *Eur. Polym. J.* **2011,** *47*, 187-195.

40. Guillem, B.; Darcos, V.; Lapinte, V.; Monge, S.; Coudane, J.; Robin, J. J., Synthesis and evaluation of triazole-linked poly(ε-caprolactone)-graft-poly(2-methyl-2-oxazoline) copolymers as potential drug carriers. *Chem. Comm.* **2012,** *48*, 2879-2881.

41. Wilcox, D. E., Isothermal titration calorimetry of metal ions binding to proteins: An overview of recent studies. *Inorg. Chim. Acta* **2008,** *361* (4), 857-867.

42. Karlsen, V.; Heggset, E. B.; Sorlie, M., The use of isothermal titration calorimetry to determine the thermodynamics of metal ion binding to low-cost sorbents. *Thermochim. Acta* **2010,** *501* (1-2), 119-121.

43. Nash, K. L., The Chemistry of TALSPEAK: A Review of the Science. *Solvent Extr. Ion Exch.* **2015,** *33* (1), 1-55.

44. Galhoum, A. A.; Mahfouz, M. G.; Abdel-Rehem, S. T.; Gomaa, N. A.; Atia, A. A.; Vincent, T.; Guibal, E., Diethylenetriamine-functionalized chitosan magnetic nano-based particles for the sorption of rare earth metal ions [Nd(III), Dy(III) and Yb(III)]. *Cellulose* **2015,** *22* (4), 2589-2605.

45. Archer, W. R.; Fiorito, A.; Heinz-Kunert, S. L.; MacNicol, P. L.; Winn, S. A.; Schulz, M. D., Synthesis and rare-earth-element chelation properties of linear poly(ethylenimine methylenephosphonate). *Macromolecules* **2020,** *53* (6), 2061-2068.

46. Torab-Mostaedi, M.; Asadollahzadeh, M.; Hemmati, A.; Khosravi, A., Biosorption of lanthanum and cerium from aqueous solutions by grapefruit peel: equilibrium, kinetic and thermodynamic studies. *Res. Chem. Intermed.* **2015,** *41* (2), 559-573.

47. Miguirditchian, M.; Guillaneux, D.; Guillaumont, D.; Moisy, P.; Madic, C.; Jensen, M. P.; Nash, K. L., Thermodynamic study of the complexation of trivalent actinide and lanthanide cations by ADPTZ, a tridentate N-donor ligand. *Inorg. Chem.* **2005,** *44* (5), 1404-1412.

48. Vasylechko, V. O.; Stechynska, E. T.; Stashkiv, O. D.; Gryshchouk, G. V.; Patsay, I. O., Sorption of Neodymium and Gadolinium on transcarpathian clinoptilolite. *Acta Phys. Pol., A* **2018,** *133* (4), 794-797.

49. Ponou, J.; Wang, L. P.; Dodbiba, G.; Okaya, K.; Fujita, T.; Mitsuhashi, K.; Atarashi, T.; Satoh, G.; Noda, M., Recovery of rare earth elements from aqueous solution obtained from Vietnamese clay minerals using dried and carbonized parachlorella. *J. Environ. Chem. Eng.* **2014,** *2* (2), 1070-1081.

50. Naser, A. A.; El-Deen, G. E. S.; Bhran, A. A.; Metwally, S. S.; El-Kamash, A. M., Elaboration of impregnated composite for sorption of Europium and Neodymium ions from aqueous solutions. *J. Ind. Eng. Chem.* **2015,** *32*, 264-272.

51. Mohamed, W. R.; Metwally, S. S.; Ibrahim, H. A.; El-Sherief, E. A.; Mekhamer, H. S.; Moustafa, I. M. I.; Mabrouk, E. M., Impregnation of task-specific ionic liquid into a solid support for removal of neodymium and gadolinium ions from aqueous solution. *J. Mol. Liq.* **2017,** *236*, 9-17.

52. Ogata, T.; Narita, H.; Tanaka, M., Adsorption behavior of rare earth elements on silica gel modified with diglycol amic acid. *Hydrometallurgy* **2015,** *152*, 178-182.

53. Demey, H.; Lapo, B.; Ruiz, M.; Fortuny, A.; Marchand, M.; Sastre, A. M., Neodymium recovery by chitosan/iron(III) hydroxide ChiFer(III) Sorbent Material: batch and column systems. *Polymers* **2018,** *10* (2), 204.

54. Elsalamouny, A. R.; Desouky, O. A.; Mohamed, S. A.; Galhoum, A. A.; Guibal, E., Uranium and neodymium biosorption using novel chelating polysaccharide. *Int. J. Biol. Macromol.* **2017,** *104*, 963-968.

55. Vlachou, A.; Symeopoulos, B. D.; Koutinas, A. A., A comparative study of neodymium sorption by yeast cells. *Radiochim. Acta* **2009,** *97* (8), 437-441.

56. Gok, C., Neodymium and samarium recovery by magnetic nano-hydroxyapatite. *J. Radioanal. Nucl. Chem.* **2014,** *301* (3), 641-651.

57. Jain, V. K.; Handa, A.; Sait, S. S.; Shrivastav, P.; Agrawal, Y. K., Pre-concentration, separation and trace determination of lanthanum(III), cerium(III), thorium(IV) and uranium(VI) on polymer supported o-vanillinsemicarbazone. *Anal. Chim. Acta* **2001,** *429* (2), 237-246.

58. Awual, M. R.; Yaita, T.; Shiwaku, H., Design a novel optical adsorbent for simultaneous ultra-trace cerium(III) detection, sorption and recovery. *Chem. Eng. J.* **2013,** *228*, 327-335.

59. Sofronov, D.; Krasnopyorova, A.; Efimova, N.; Oreshina, A.; Bryleva, E.; Yuhno, G.; Lavrynenko, S.; Rucki, M., Extraction of radionuclides of cerium, europium, cobalt and strontium with Mn3O4, MnO2, and MNOOH sorbents. *Process Saf. Environ. Prot.* **2019,** *125*, 157-163.

60. Sadovsky, D.; Brenner, A.; Astrachan, B.; Asaf, B.; Gonen, R., Biosorption potential of cerium ions using Spirulina biomass. *J. Rare Earths* **2016,** *34* (6), 644-652.

61. Sert, S.; Kuetahyali, C.; Inan, S.; Talip, Z.; Cetinkaya, B.; Eral, M., Biosorption of lanthanum and cerium from aqueous solutions by Platanus orientalis leaf powder. *Hydrometallurgy* **2008,** *90* (1), 13-18.